Surface modification of nitrogen-doped carbon quantum dots for enhanced functionalities

Pham Van Duong 1 , Nguyen Minh Hoa 2 , Do Minh Hieu 1 , Le Thi Thu Huong 1 , Nguyen Duc Toan 1 , Pham Hong Minh 1 , Nguyen Trong Tuyen 3 , Nguyen Dinh Lam 4 , Le Anh Thi 5,6 , Nguyen Thanh Binh 1,†

E-mail: †tbnguyen@iop.vast.vn

Received 9 September 2024; Accepted for publication 12 December 2024 Published 19 December 2024

Abstract. A facile and controllable one-step atmospheric pressure microplasma method was employed to synthesize nitrogen-doped carbon quantum dots with tunable optical properties. The nitrogen-doped carbon quantum dots were characterized using Fourier transform infrared spectroscopy, high-resolution transmission electron microscopy, UV–Vis absorption spectroscopy, and photoluminescence spectroscopy. High-resolution transmission electron microscopy revealed uniformly distributed spherical nanoparticles with a graphite-like structure. Fourier transform infrared spectroscopy confirmed effective nitrogen doping, enhancing chemical stability. UV–Vis spectroscopy revealed redshifted absorption peaks, indicating improved electronic interactions and a reduced bandgap (4.05 eV) compared to those of undoped carbon quantum dots (4.18 eV). Photoluminescence analysis revealed excitation-dependent emission and a significantly higher photoluminescence quantum yield of 33.09%. These results suggest that nitrogen-doped carbon quantum dots hold promise for applications in optoelectronics and bioimaging, providing a foundation for further optimization in future studies.

©2024 Vietnam Academy of Science and Technology

¹Institute of Physics, Vietnam Academy of Science and Technology, 10 Dao Tan, Ba Dinh, Hanoi 10000, Vietnam

²Faculty of Fundamental Sciences, Hue University of Medicine and Pharmacy, Hue University, Hue, Vietnam

³Vietnam-Hungary Industrial University, 16 Xuan Khanh, Son Tay, Hanoi 10000, Vietnam

⁴Faculty of Engineering Physics and Nanotechnology,

VNU-University of Engineering and Technology Hanoi, 11310, Vietnam

⁵Institute of Research and Development, Duy Tan University, Da Nang 550000, Vietnam

⁶Faculty of Natural Sciences, Duy Tan University, Da Nang 550000, Vietnam

Keywords: Microplasma; nitrogen-doped carbon quantum dots; optical properties; surface modification.

Classification numbers: 81.05.U-; 81.05.uj; 68.35.bm; 52.77.Bn; 73.20.Mf; 52.40.-w..

1. Introduction

The development of photoluminescent nanomaterials has revolutionized the field of fluorescent materials [1–4]. Among the various options being explored, such as semiconductor nanocrystals, metal complexes, and carbon-based materials, carbon-based materials have gained significant attention. This is due to their unique advantages, including biocompatibility, simple synthesis, low cost, photostability, and environmental friendliness [2, 5–8]. However, inducing luminescence in carbon-based materials has been challenging. Traditional forms of carbon, such as graphite and diamond, do not readily emit light due to the conductivity of graphite and the wide indirect bandgap of 5.5 eV of diamond [9]. Nonetheless, the advent of nanostructuring has provided a solution. Carbon nanostructures, such as single- and multi-walled carbon nanotubes and fullerenes, possess unique properties that allow for efficient light emission despite these limitations [10, 11].

Xiaoyou Xu and colleagues made significant breakthroughs in the discovery of carbon quantum dots (CQDs) in 2004 [12]. These nanomaterials, which are typically smaller than 10 nm, feature a sp² hybridized graphitic core with a functionalized surface [7,13]. Research has focused on understanding their unique photoluminescence (PL), which is influenced by their chemical structure, core properties, and surface functionalities [14,15]. Despite proposed mechanisms such as size distribution, surface states, and exciton recombination, the exact origins of CQD light emission are not fully understood due to limited theoretical models and data. Key questions include whether CQDs can be controlled or modified to tailor light emissions, expanding their applications [1,2]. Investigating the binding properties of CQDs with ligands and enhancing their photophysical properties through chemical and physical modifications are crucial for broader applications [1,8]. Techniques such as surface functionalization, core-shell design, and heteroatom doping (sulfur, nitrogen, boron, phosphorus) are promising, particularly nitrogen doping, because of its effective interaction with carbon atoms, enabling precise control of the PL properties of CQDs [16].

Nitrogen plays a crucial role in CQDs synthesis as a key charge carrier atom [17]. With an atomic radius comparable to that of carbon and five valence electrons in its outermost shell, nitrogen forms strong bonds with carbon atoms within the CQDs structure [18, 19]. Importantly, nitrogen functions as an n-type donor atom, readily donating electrons to the CQDs system. During excitation, these electrons can transfer to the lowest unoccupied molecular orbital of the substrate, quenching the self-fluorescence of the CQDs [17,20]. This quenching effect, influenced by the abundance of n-type nitrogen on CQDs surfaces, broadens their analytical range and enhances their detection capabilities, bolstering their potential for various applications [20–22]. The modification of CQDs PL via nitrogen doping has been reported to significantly improve quantum yields and photostability, as shown in recent studies [23].

Various synthesis methods including chemical-only methods, hydrothermal and solvothermal processes, oxidative acid treatments, microwave treatments, laser ablation, and electrochemical methods, are used to produce CQDs with tunable optical properties and high quantum yields [7, 24–27]. Achieving precise particle sizes often requires post-synthesis treatments such as washing

and annealing, which can be time- and energy-intensive, posing challenges for scalability and reproducibility. An alternative method uses plasma-liquid discharge energy to activate precursors without requiring thermal or chemical energy, making it suitable for temperature-sensitive or low-reactivity precursors. This approach enables the functionalization and doping of CQDs through plasma-induced nonequilibrium electrochemistry methods, producing CQDs with strong luminescence. Low-temperature and low-power synthesis methods, such as microplasma synthesis, are preferred for applications where preserving surface functional groups is crucial for maintaining luminescence [28]. More recent work has intensified reactivity using a bespoke plasma system, demonstrating that transient hydrodynamics can enhance reaction rates, improve mass yield, and increase process efficiency for large-scale production of nitrogen-doped carbon quantum dots (N-CQDs) [29].

In previous research, we synthesized CQDs using atmospheric pressure microplasma and evaluated their antibacterial activities [30,31]. Expanding on this research, we conducted experimental investigations to examine the electronic transitions within N-CQDs. Our findings highlight that these electronic transitions primarily originate from nitrogen-doped sites within N-CQDs. By utilizing our synthesis method to control substitutional versus surface doping without impacting the quantum dot morphology, we systematically explored the complex relationships among the structure, chemical composition, and emission properties of N-CQDs. This study significantly enhances our understanding of N-CQD properties, elucidating changes in PL emission and the critical role of N-CQD absorption in promoting exciton radiative recombination. These insights are essential for advancing the applications of N-CQDs in optoelectronic devices.

2. Experiment

N-CQDs were synthesized via a plasma method using acetone and ammonia as precursors, as shown in Fig. 1. Acetone provided the carbon source, while ammonia introduced nitrogen doping. The plasma reactor enabled controlled reactions under specific temperature and pressure conditions. Throughout the synthesis process, the precursor mixture underwent plasma discharge to promote the formation of N-CQDs. Following synthesis, the product was purified through centrifugation and dialysis to eliminate any remaining precursors and byproducts.

The synthesized N-CQDs underwent comprehensive characterization using various analytical techniques. High-resolution transmission electron microscopy (HRTEM) was employed to analyze their morphology and size distribution. Fourier transform infrared spectroscopy (FTIR) was conducted using a JASCO 6700 spectrometer to identify functional groups in both CQDs and N-CQDs. UV-visible spectrophotometry (UV-Vis-Xplorer) was used to examine absorption spectra across the 200-800 nm range. PL spectroscopy and lifetime measurements were performed using a FLS 1000, Edinburgh fluorescence spectrophotometer to evaluate their photoluminescent properties.

3. Results and discussion

3.1. Morphological analysis of the CQDs and N-CQDs

Figure 2 presents TEM images of CQDs and HRTEM images of N-CQDs, illustrating their spherical nanoparticle morphology with uniform distribution and no agglomeration. The size distribution of CQDs ranges from 2 to 10 nm, averaging approximately 5.7 nm, while N-CQDs

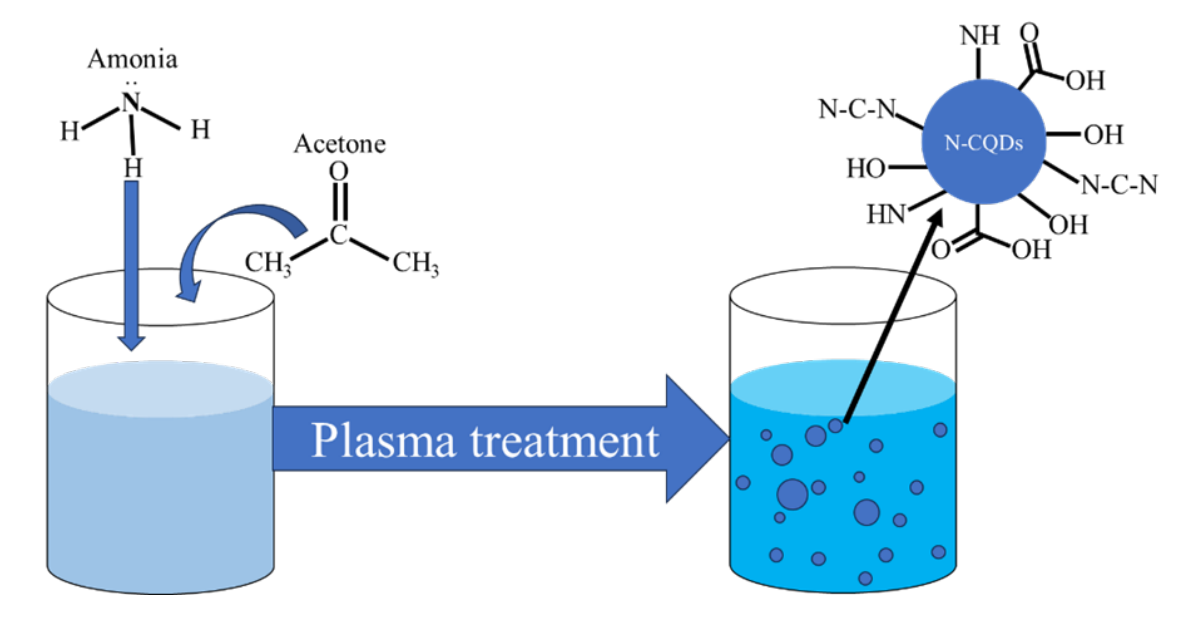


Fig. 1. Schematic of the N-doped CQD synthesis process.

range from 2 to 8.2 nm, averaging about 5.8 nm (see insets in Fig. 2a and 2b). HRTEM images of N-CQDs show clear lattice fringes, with an inset revealing stripe-like structures and a lattice spacing of 0.23 nm, indicative of a graphite-like structure similar to the (100) diffraction facet of graphitic carbon [22].

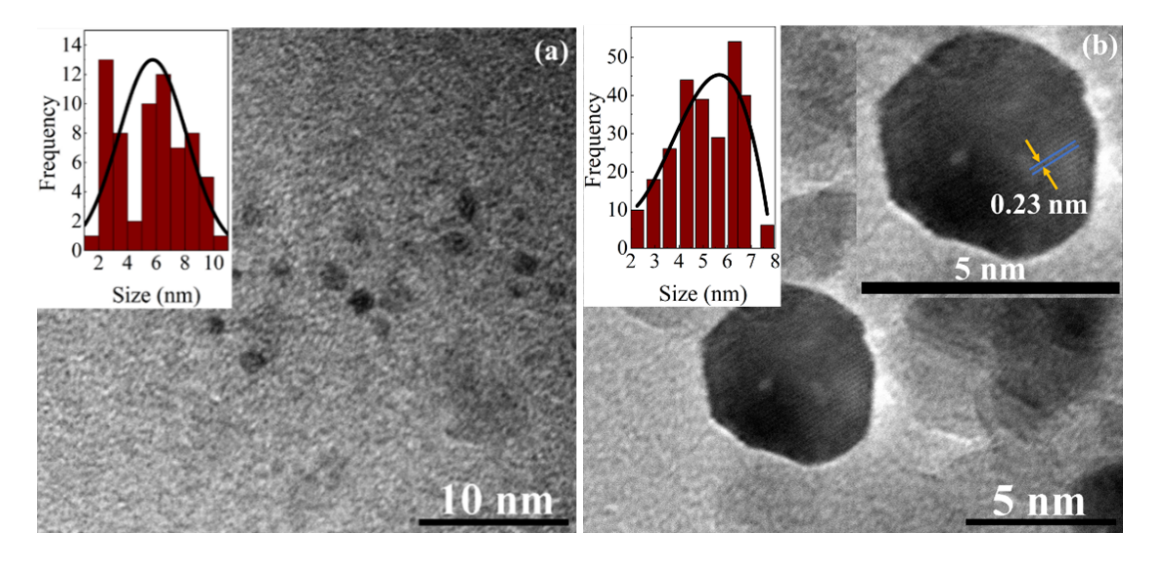


Fig. 2. (a) TEM images of the CQDs (inset: size distribution); (b) HRTEM images of the N-CQDs (inset: size distribution (left side)) and lattice fringes (right side).

3.2. FTIR spectroscopy

To identify functionalization, FTIR spectroscopy was applied to analyze synthesized CQDs and N-CQDs. In Figure 3, CQDs exhibit characteristic absorption peaks at 2974 cm⁻¹ and 902 cm⁻¹ (C-H stretching), 1353 cm⁻¹ (C=O), and 1215 cm⁻¹ (C-O). Both CQDs and N-CQDs show a peak at 1707 cm⁻¹, indicating unsaturated C=C bonds consistent with the literature [20,21]. The N-CQDs spectrum displays distinctive peaks at 1468 cm⁻¹ (C-N stretching) and bands between 902 cm⁻¹ and 3257 cm⁻¹, indicating N-H bending and heterocyclic C-N-C bond stretching vibrations at 1148 cm⁻¹ and 1177 cm⁻¹ [17, 22]. Reduced C-O stretching at 1215 cm⁻¹ and enhanced C-N vibrations at 1468 cm⁻¹ confirm the successful incorporation of N-containing groups via chemical reaction, likely involving ethylenediamine and microcrystalline cellulose [17, 18]. This illustrates the efficient doping of nitrogen species into the CQDs structure.

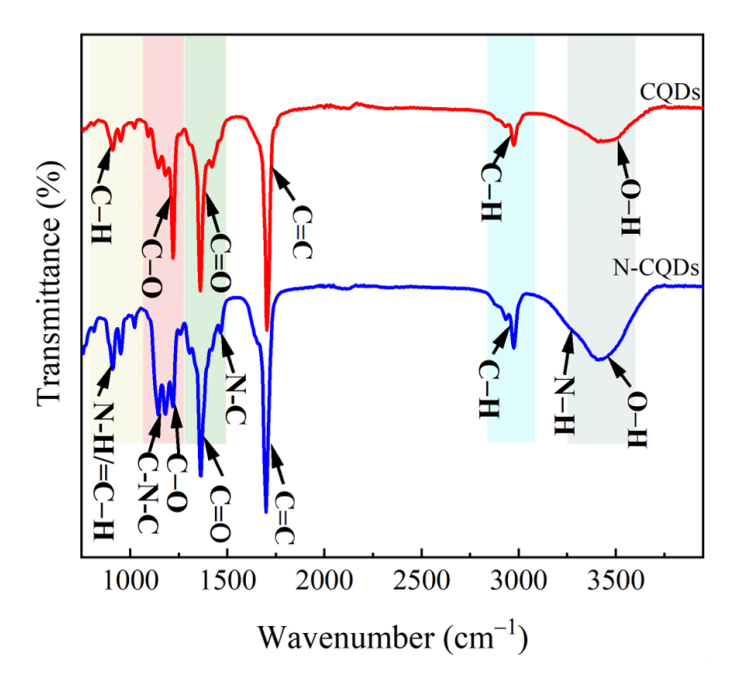


Fig. 3. FTIR spectra of CQDs and N-CQDs.

3.3. Optical properties of the CQDs and N-CQDs

The UV-Vis absorption spectra of both CQDs and N-CQDs exhibit absorption bands in the ultraviolet region, attributed to the aromatic π -system (Fig. 4a). The main peaks are observed around 280 nm, with an additional shoulder peak near 350 nm, which correspond to π - π^* transitions within sp² domains and $n-\pi^*$ transitions involving surface bonds such as C=O, C-N, and C=N [17, 20]. Notably, N-CQDs show a shift towards longer wavelengths compared to undoped CQDs, indicating enhanced electronic interactions likely due to nitrogen incorporation. This change suggests the introduction of additional electronic states or an increased density of states contributed by nitrogen doping. The Tauc plots, presented in Figure 4b, reveal direct bandgap values of E_g = 4.18 eV for CQDs and E_g = 4.05 eV for N-CQDs, highlighting alterations

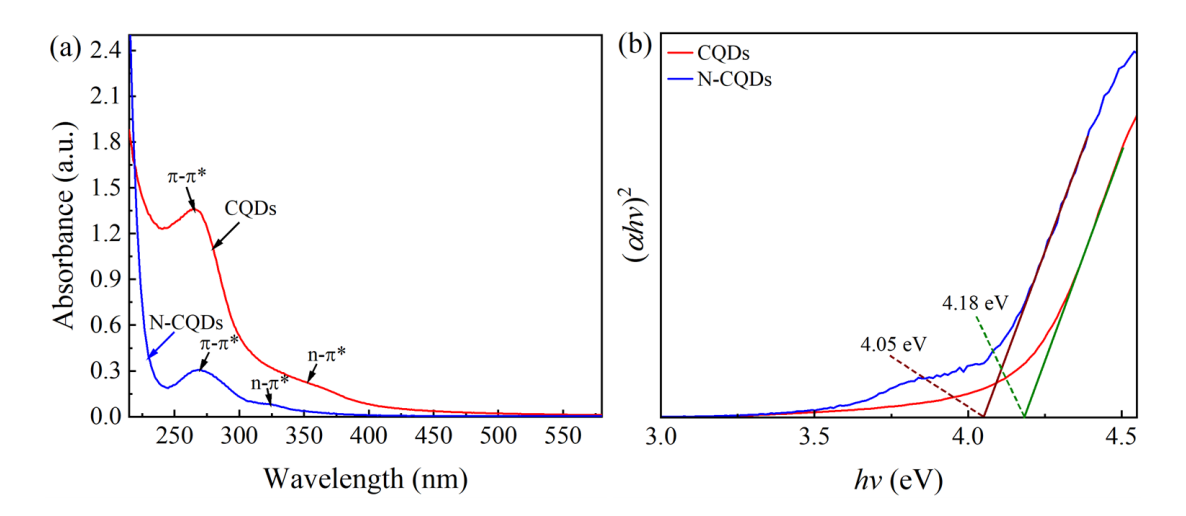


Fig. 4. (a) UV–Vis absorption spectra and (b) Tauc plots of the CQDs and N-CQDs.

in the optical and electronic properties induced by nitrogen doping. Graphitic nitrogen and surface nitrogen atoms contain lone pairs of electrons, which contribute to a positive charge by donating electrons to the carbon structure. This electron donation increases the electron density, leading to a reduction in the bandgap. As a result, the electronic structure of the N-CQDs and their absorption tails are influenced by charge transfer and frontier orbital hybridization between the carbon core and surface functional groups [18].

The PL spectra with an excitation wavelength of 410 nm show a distinct difference between the CQDs and N-CQDs aqueous solutions as depicted in Figure 5a, the fluorescence emission intensity of N-CQDs is not only stronger than that of the CQDs at the same concentration but a blue shift in the maximum PL wavelength is also observed. This enhancement can be attributed to a reduction in non-radiative recombination centers on the N-CQDs surface [32]. The PL spectra of both CQDs and N-CQDs were measured at excitation wavelengths ranging from 390 to 490 nm in 10 nm increments, as depicted in Figures 5b and 5c. Each sample demonstrated excitation-dependent emission behavior, advantageous for applications like biosensors, bioimaging, and LED devices. Emission peaks varied with excitation wavelengths, suggesting unique optimal conditions for each sample. Overall, the PL study underscored the intriguing optical properties of N-CQDs. The results affirmed previous findings of excitation-dependent emission in CQDs [33, 34]. At an excitation wavelength of 420 nm, CQDs exhibit a maximum emission at 508 nm (Fig. 5b), while N-CQDs show a maximum at 513 nm (Fig. 5c). The PL intensity for both types of quantum dots increases from 390 to 420 nm but then gradually decreases as the excitation wavelength shifts from 430 to 490 nm. This behavior is attributed to the electronegativity of heteroatoms, quantum confinement effects, and the presence of surface traps on the CQDs. The excitation-dependent emissions are mainly due to the different functional groups, such as nitrogen and oxygen, present on the surface of N-CQDs, which provide various emissive sites. However, the exact mechanisms behind these properties remain unclear. The quantum confinement effect is commonly cited, linked to CQDs' broad particle size distribution influencing energy gaps and emission wavelengths [19, 34]. HRTEM analysis indicated that increased nitrogen doping did not

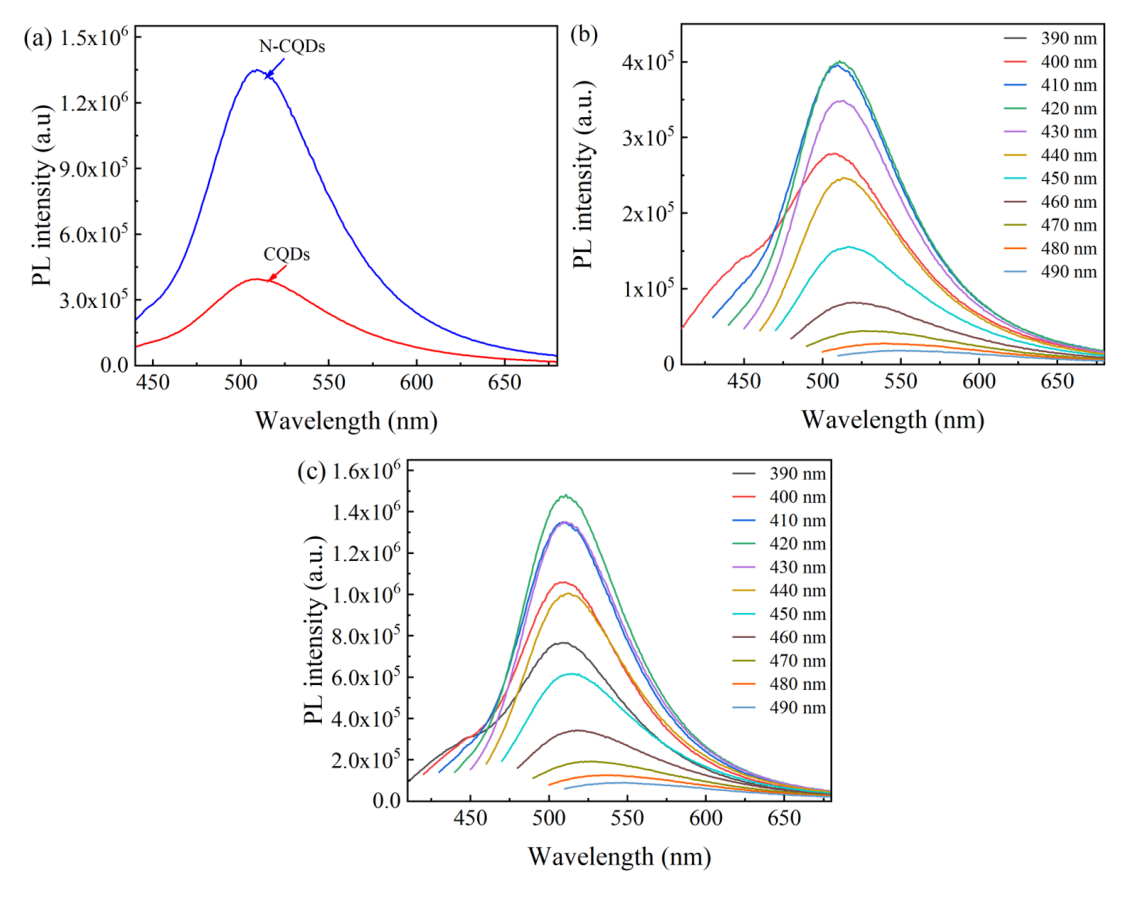


Fig. 5. (a) PL spectra of the CQDs and N-CQDs under maximum excitation at 410 nm and emission spectra of the (b) CQDs and (c) N-CQDs under different excitation wavelengths.

alter particle size, suggesting the redshift in emission arises from radiative recombination within sp² clusters rather than the size effect [17]. Surface state theory was also considered, supported by UV–Vis absorbance showing a peak at 265 nm, indicative of $\pi - \pi^*$ transitions and significant π -electron presence. Surface oxidation potentially interacts with these π -electrons with surface electronic states, modifying N-CQDs' electronic structure [17].

The photoluminescence lifetimes and quantum yields of both CQDs and N-CQDs were meticulously measured to delve into their photoluminescence characteristics. The decay curves are adeptly fitted using a multiexponential function. This approach facilitates a comprehensive analysis of the decay dynamics, capturing multiple contributing factors to the fluorescence decay process [35].

$$I(t) = A_1 \exp(-t/\tau_1) + A_2 \exp(-t/\tau_2), \tag{1}$$

where A_1 , A_2 represent the amplitudes, while τ_1 , τ_2 represent the time constants associated with each exponential component. This multiexponential fitting approach augments our understanding of the intricate fluorescence decay kinetics of CQDs, providing insights into the underlying

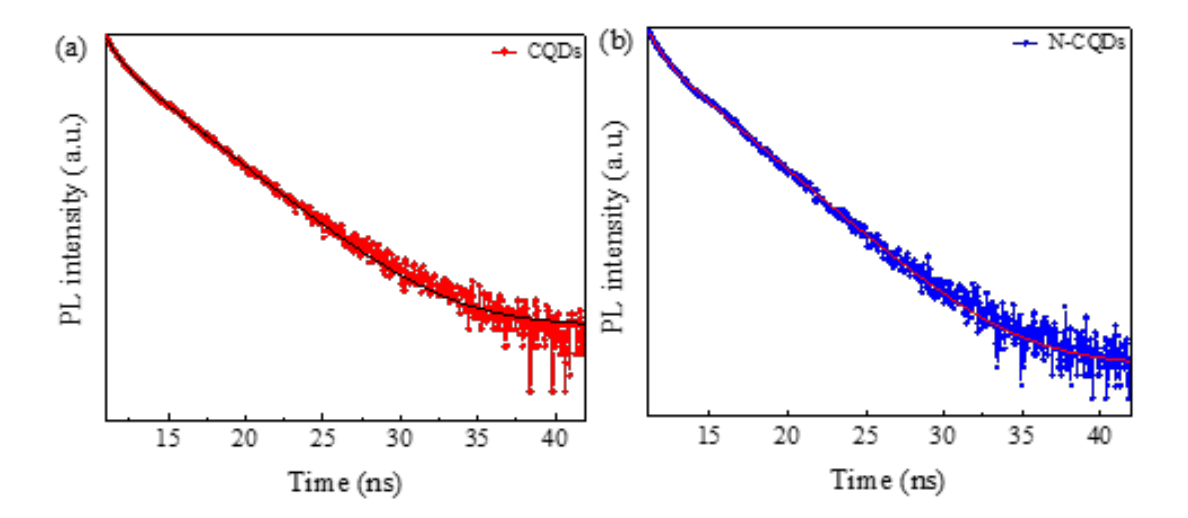


Fig. 6. Photoluminescence lifetimes of CQDs and N-CQDs.

processes governing their temporal behavior. The average lifetime (τ_{avg}) is calculated by the following $\tau_{avg} = (A_1\tau_1^2 + A_2\tau_2^2)/(A_1\tau_1 + A_1\tau_1)$. The results presented in Table 1 indicate a notable enhancement in both PL lifetime and PLQY with the introduction of nitrogen doping. Specifically, N-CQDs exhibited a significantly higher photoluminescence quantum yield (PLQY) of 33.09% compared to 22.71% for CQDs, as shown in Table 1. The PLQY of N-CQDs was also compared with those reported in other publications. These findings underscore the efficacy of nitrogen doping in improving the efficiency of photoluminescence in the synthesized N-CQDs, thereby enhancing their potential for applications in optoelectronic devices and other photonics-related fields.

Table 1. A significant reduction in nonradiative rates was observed in CQDs and N-CQDs.

Samples	A_1	A_2	$ au_1$	$ au_2$	τ _{avg} (%)	PLQY kr (ns-1)	Radiative knr (ns-1)	Nonradiative
CQDs	0.53	0.69	0.76	3.39	3.00	22.71 33.09 33 ^a	0.076	0.105
N-CQDs	0.34	0.70	0.65	3.37	3.14	13 ^b 14.21 ^c 14.0 ^d 9.6 ^e	0.257	0.212

^a [17]; ^b [32]; ^c [20]; ^d [36]; ^e [37]

The radiative rate (k_r) and nonradiative rate (k_{nr}) were determined using Eqs. (2) and (3) [18]:

$$k_r = \frac{\Phi}{\tau},\tag{2}$$

$$k_{nr} = \frac{1 - \Phi}{\tau},\tag{3}$$

where Φ represents the PLQY of the samples and τ is the lifetime at which the fluorescence diminishes to 1/e of its initial value.

The significant reduction in nonradiative rates observed in N-CQDs, as depicted in Table 1 and Fig. 6, highlights their enhanced PL performance. This decrease indicates that fewer excited states decay non-radiatively, resulting in a higher photoluminescence quantum yield (PLQY). The presence of nitrogen functional groups on the N-CQDs surface is pivotal as they effectively passivate surface defects, thereby boosting radiative recombination efficiency. The nanosecond-scale PL lifetime observed further validates this efficient radiative recombination process, which is crucial for applications requiring prolonged emission and superior PLQY [18, 20, 21].

4. Conclusion

We successfully synthesized N-CQDs via a plasma process using acetone as the carbon source and ammonia for nitrogen doping. These N-CQDs demonstrated excellent optical properties, achieving a high photoluminescence quantum yield of approximately 33.09%. The UV-Vis spectra revealed a redshifted absorption peak in the N-CQDs, indicating enhanced electronic interactions and a reduced bandgap (4.05 eV) compared to undoped CQDs (4.18 eV). Fluorescence lifetime studies confirmed that the reduced nonradiative recombination rates are due to surface passivation and the inner filter effect. This study presents a rapid, single-step, and environmentally friendly approach for synthesizing high-performance carbon-based nanomaterials, offering significant potential for applications in optoelectronics, bioimaging and sensing.

Acknowledgments

This work is supported by the Program for Physics Development at the Vietnam Academy of Science and Technology (VAST) under Project No. KHCBVL.05/23-24. The authors are grateful for the use of the facilities of the Joint Optics and Photonics Laboratory at the Institute of Physics (IOP, VAST). Minh Hieu Do also wishes to thank the institutional project of the Institute of Physics for its support in 2024.

Authors contributions

P. V. Duong, L. A. Thi, and D. M. Hieu conceived the experiment. P. H. Minh, L. T. T. Huong, N. D. Toan, N. T. Tuyen, and N. M. Hoa conducted the experiments and analyzed the data; P. V. Duong, N. T. Binh, and N. M. Hoa, N. D. Lam wrote the initial draft of the paper. N. T. Binh and P. V. Duong supervised the work. All authors participated in the discussion of the results; All authors have read and agreed to the published version of the manuscript.

Conflict of interest

The authors declare that they have no known competing financial interests or personal relationships that could have appeared to influence the work reported in this paper.

References

- [1] A. Kolanowska, G. Dzido, M. Krzywiecki, M. M. Tomczyk, D. Łukowiec, S. Ruczka and S. Boncel, *Carbon quantum dots from amino acids revisited: survey of renewable precursors toward high quantum-yield blue and green fluorescence*, ACS Omega 7 (2022) 41165.
- [2] B. K. John, T. Abraham and B. Mathew, A review on characterization techniques for carbon quantum dots and their applications in agrochemical residue detection, J. Fluoresc. 32 (2022) 449.
- [3] S. Zhang, C. Xiao, H. He, Z. Xu, B. Wang, X. Chen et al., The adsorption behaviour of carbon nanodots modulated by cellular membrane potential, Environ. Sci. Nano 7 (2020) 880.
- [4] K. A. S. Fernando, S. Sahu, Y. Liu, W. K. Lewis, E. A. Guliants, A. Jafariyan et al., Carbon quantum dots and applications in photocatalytic energy conversion, ACS Appl. Mater. Interfaces 7 (2015) 8363.
- [5] N.K. Stanković, M. Bodik, P. Šiffalovič, M. Kotlar, M. Mičušik, Z. Špitalsky, M. Danko, D.D. Milivojević, A. Kleinova, P. Kubat, Z. Capakova, P. Humpoliček, M. Lehocky, B.M. Todorović Marković, Z.M. Marković, Antibacterial and antibiofouling properties of light triggered fluorescent hydrophobic carbon quantum dots langmuir-blodgett thin films, ACS Sustain. Chem. Eng. 6 (2018) 4154.
- [6] Z.M. Marković, M. Kováčová, P. Humpolíček, M.D. Budimir, J. Vajďák, P. Kubát, M. Mičušík, H. Švajdlenková, M. Danko, Z. Capáková, M. Lehocký, B.M. Todorović Marković, Z. Špitalský, Antibacterial photodynamic activity of carbon quantum dots/polydimethylsiloxane nanocomposites against Staphylococcus aureus, Escherichia coli and Klebsiella pneumoniae, Photodiagnosis Photodyn. Ther. 26 (2019) 342.
- [7] X. Ma, S. Li, V. Hessel, L. Lin, S. Meskers and F. Gallucci, Synthesis of luminescent carbon quantum dots by microplasma process, Chem. Eng. Process. - Process Intensif. 140 (2019) 29.
- [8] S. Pandiyan, L. Arumugam, S. P. Srirengan, R. Pitchan, P. Sevugan, K. Kannan et al., Biocompatible Carbon Quantum Dots Derived from Sugarcane Industrial Wastes for Effective Nonlinear Optical Behavior and Antimicrobial Activity Applications, ACS Omega 5 (2020) 30363.
- [9] F. Zhao, X. Li, M. Zuo, Y. Liang, P. Qin, H. Wang et al., Preparation of photocatalysts decorated by carbon quantum dots (CQDs) and their applications: A review, J. Environ. Chem. Eng. 11 (2023) 109487.
- [10] N. Arora and N.N. Sharma, Arc discharge synthesis of carbon nanotubes: Comprehensive review, Diam. Relat. Mater. 50 (2014) 135.
- [11] A. J. Clancy, M. K. Bayazit, S. A. Hodge, N. T. Skipper, C. A. Howard and M. S. P. Shaffer, Charged Carbon Nanomaterials: Redox Chemistries of Fullerenes, Carbon Nanotubes, and Graphenes, Chem. Rev. 118 (2018) 7363
- [12] X. Xu, R. Ray, Y. Gu, H.J. Ploehn, L. Gearheart, K. Raker, W.A. Scrivens, Electrophoretic analysis and purification of fluorescent single-walled carbon nanotube fragments, J. Am. Chem. Soc. 126 (2004) 12736.
- [13] Y. Hou, Q. Lu, J. Deng, H. Li, Y. Zhang, One-pot electrochemical synthesis of functionalized fluorescent carbon dots and their selective sensing for mercury ion, Anal. Chim. Acta 866 (2015) 69.
- [14] N. K. Quang, N. N. Hieu, V. V. Q. Bao, V. T. Phuoc, L. X. D. Ngoc, L. Q. Doc, et al., *Hydrothermal synthesis of carbon nanodots from wine cork and biocompatible fluorescent probe*, Beilstein Arch. **2021** (2021) 202145.
- [15] Z. Sun, F. Yan, J. Xu, H. Zhang and L. Chen, Solvent-controlled synthesis strategy of multicolor emission carbon dots and its applications in sensing and light-emitting devices, Nano Res. 15 (2022) 414.
- [16] X. Ma, S. Li, V. Hessel, L. Lin, S. Meskers and F. Gallucci, Synthesis of N-doped carbon dots via a microplasma process, Chem. Eng. Sci. 220 (2020) 115648.
- [17] S. D. Dsouza, M. Buerkle, P. Brunet, C. Maddi, D. B. Padmanaban, A. Morelli et al., The importance of surface states in N-doped carbon quantum dots, Carbon N. Y. 183 (2021) 1.
- [18] X. Dong, H. Qi, Z. Zhai, W. Li, P. Zhang, Probing the fluorescence quenching mechanism of N-doped carbon quantum dots by inorganic ions, Microchem. J. 197 (2024) 109854.
- [19] R. Shi, Z. Li, H. Yu, L. Shang, C. Zhou, G.I.N. Waterhouse, L.Z. Wu, T. Zhang, Effect of nitrogen doping level on the performance of n-doped carbon quantum dot/TiO₂ Composites for Photocatalytic Hydrogen evolution, ChemSusChem 10 (2017) 4650.
- [20] Rishabh, M. Rani, U. Shanker, B. Singh Kaith and M. Sillanpää, Green fabrication of fluorescent N-doped carbon quantum dots from Aegle marmelos leaves for highly selective detection of Fe³⁺ metal ions, Inorg. Chem. Commun. 159 (2024) 111878.

- [21] X. J. Jiang, Y. Ma, Y. Zhou, R. D. Xiao, Y. J. Meng, Ye-Hou et al., Green one-step synthesis of N-doped carbon quantum dots for fluorescent detection of lemon yellow in soft drinks, Spectrochim. Acta - Part A Mol. Biomol. Spectrosc. 316 (2024) 124305.
- [22] X. Luo, P. Bai, X. Wang, G. Zhao, J. Feng and H. Ren, *Preparation of nitrogen-doped carbon quantum dots and its application as a fluorescent probe for Cr(VI) ion detection*, New J. Chem. **43** (2019) 5488.
- [23] Q. H. Pho, L. L. Lin, N. N. Tran, T. T. Tran, A. H. Nguyen, D. Losic et al., Rational design for the microplasma synthesis from vitamin B9 to N-doped carbon quantum dots towards selected applications, Carbon N. Y. 198 (2022) 22.
- [24] X. Qin, W. Lu, A.M. Asiri, A.O. Al-Youbi and X. Sun, Microwave-assisted rapid green synthesis of photoluminescent carbon nanodots from flour and their applications for sensitive and selective detection of mercury(II) ions, Sens. Actuators B Chem. 184 (2013) 156.
- [25] M. Fu, F. Ehrat, Y. Wang, K.Z. Milowska, C. Reckmeier, A.L. Rogach, J.K. Stolarczyk, A.S. Urban, J. Feldmann, Carbon Dots: A Unique Fluorescent Cocktail of Polycyclic Aromatic Hydrocarbons, Nano Lett. 15 (2015) 6030.
- [26] Z. Yan, J. Shu, Y. Yu, Z. Zhang, Z. Liu and J. Chen, *Preparation of carbon quantum dots based on starch and their spectral properties*, Luminescence **30** (2015) 388.
- [27] P. Yang, Z. Zhu, T. Zhang, M. Chen, Y. Cao, W. Zhang et al., Facile synthesis and photoluminescence mechanism of green emitting xylose-derived carbon dots for anti-counterfeit printing, Carbon N. Y. 146 (2019) 636.
- [28] Q. H. Pho, L. L. Lin, E. V. Rebrov, M. Mohsen Sarafraz, T. T. Tran, N. N. Tran, D. Losic, V. Hessel, Process intensification for gram-scale synthesis of N-doped carbon quantum dots immersing a microplasma jet in a gasliquid reactor, Chem. Eng. J. 452 (2023) 139164.
- [29] Q. Hue Pho, V. Hessel, E. V. Rebrov, N. Van Duc Long, P. Lamichhane, N. Nghiep Tran, D. Losic, Stagnant liquid layer as "Microreaction System" in submerged plasma Micro-Jet for formation of carbon quantum dots, Chem. Eng. J. 495 (2024) 153571.
- [30] M.H. Nguyen, D.T. Le, H.T. Do, A.T. Le, Remarkable luminescent carbon quantum dots: green synthesis from orange juice using microplasma-liquid method, Fullerenes Nanotub. Carbon Nanostructures 32 (2024) 282.
- [31] M. H. Nguyen, A. T. Le, V. D. Pham, H. M. Pham, H. T. Do, D. T. Le et al., TA Comprehensive study on the antibacterial activities of carbon quantum dots derived from orange juice against Escherichia coli, Appl. Sci. 14 (2024) 51.
- [32] P. Wu, W. Li, Q. Wu, Y. Liu and S. Liu, Hydrothermal synthesis of nitrogen-doped carbon quantum dots from microcrystalline cellulose for the detection of Fe³⁺ ions in an acidic environment, RSC Adv. 7 (2017) 44144.
- [33] X. Niu, Y. Li, H. Shu and J. Wang, Revealing the underlying absorption and emission mechanism of nitrogen doped graphene quantum dots, Nanoscale 8 (2016) 19376.
- [34] G. S. Jamila, S. Sajjad, S. A. K. Leghari and Y. Li, Pivotal role of N and Bi doping in CQD/Mn₃O₄ composite structure with outstanding visible photoactivity, New J. Chem. 44 (2020) 11631.
- [35] X. Feng, Y. Zhang, A simple and green synthesis of carbon quantum dots from coke for white light-emitting devices, RSC Adv. 9 (2019) 33789–33793. https://doi.org/10.1039/c9ra06946a.
- [36] K.G. Nguyen, M. Huš, I.A. Baragau, J. Bowen, T. Heil, A. Nicolaev et al., Engineering Nitrogen-Doped Carbon Quantum Dots: Tailoring Optical and Chemical Properties through Selection of Nitrogen Precursors, Small 20 (2024) 2310587.
- [37] K. G. Nguyen, I. A. Baragau, R. Gromicova, A. Nicolaev, S. A. J. Thomson, A. Rennie et al., Investigating the effect of N-doping on carbon quantum dots structure, optical properties and metal ion screening, Sci. Rep. 12 (2022) 13806.